Chemistry–A European Journal
Research Article
doi.org/10.1002/chem.202203907
Chemistry Europe
European Chemical Societies Publishing
www.chemeurj.org

Green and Fast Strategies for Energy-Efficient Preparation of the Covalent Organic Framework TpPa-1

Íñigo Martínez-Visus,[a, b] Matías Ulcuango,[a, b] Beatriz Zornoza,*[a, b] Joaquín Coronas,[a, b] and Carlos Téllez*[a, b]

Abstract: Three synthesis procedures for the covalent-organic framework (COF) TpPa-1 are studied with the purpose of setting up the most promising one in a fast and green way, leading to a more environmentally friendly and sustainable process. With conventional heating, good crystallinity and a high BET specific surface area (SSA) of up to 1007 $m^2 \cdot g^{-1}$ are achieved at 170 °C for 3 days using water as the quintessential green solvent. However, the application of microwave radiation in the synthesis for this crystalline porous polymer allows reaction times to be shortened to 30 min while maintaining structural and textural properties (BET SSA of 928 $m^2 \cdot g^{-1}$) and obtaining yields close to 98% (vs. 90% in the hydrothermal synthesis). The water-assisted mechanochemical synthesis is also an environmentally friendly synthetic approach; with heating at 170 °C in a two-step process (10 + 10 min), high crystallinity is achieved, a BET SSA of 960 $m^2 \cdot g^{-1}$ and a yield of 98% for TpPa-1.

Introduction

Covalent organic frameworks (COFs) are crystalline porous polymeric structures made by covalent bonding between light elements (H, C, B, N and O).[1] These new ordered structures assembled by versatile molecular building blocks have the potential for overcoming current challenges in the development of novel functionalized materials.[2] COFs show permanent porosity, high specific surface areas, tailored pore sizes and functionalized moieties,[3] making them suitable in a wide field of applications related to semiconductors,[4] energy and gas storage,[5] separations,[6] catalysis,[7] photocatalysis,[8] gas separation[9] and drug delivery.[10] The first imine-linked COF was synthesized by Uribe-Romo et al. in 2009[11] improving chemical and thermal stability over existing boronate ester and borosilicate linkages. β-Ketoenamine COFs like TpPa-1 are obtained by a two-step process built upon imine linkages, consisting of a reversible Schiff base reaction and an irreversible tautomerization (Figure 1). At present, the main roadblock in COF synthesis is the crystallization step, as reversible conditions for covalent bond formation are necessary for structure error-correction and achievement of high crystallinity.[12] The Schiff base condensation is a highly reversible reaction that allows the construction of an ordered structure; furthermore, the in-series irreversible keto-enol tautomerization bestows further stability and permanent properties.[13]

Although multiple ways of COF synthesis such as solvothermal,[14] ionothermal,[15] microwave,[16] mechanochemical[17] and interfacial[18] have been extensively studied, a general synthetic approach still seems desirable. Solvothermal synthesis is widely used, as it allows for good control of the reactive media to ensure correct reactivity and solubility of monomers, with the downside of long reaction times (up to nine days in some cases) at moderate temperature, the combination of various organic solvents and harsh conditions.[19] Shorter times through microwave-assisted synthesis have been achieved, reducing the COF preparation down to a few hours or even minutes, as well as obtaining higher yields and more crystalline products with a process that is itself energy efficient.[20] More sustainable and environmentally friendly procedures like hydrothermal, sonochemical[21] and solvent-free syntheses[22] for COFs have been carried out, replacing the organic solvents used in the traditional solvothermal method by greener alternatives, reducing toxicity and lowering their costs.

Banerjee's group was the first to synthesize TpPa-1 under hydrothermal conditions and other β-ketoenamine COFs,[23] showing that high crystallinity and specific surface area and porosity values could be obtained almost on par with conventional solvothermal synthesis. Moreover, mechanochemical synthesis or "organic terracotta process" was also reported by the same group[24] with interesting textural and crystalline properties in the achieved products. Additionally, TpPa-1 obtained by

[a] Í. Martínez-Visus, M. Ulcuango, Dr. B. Zornoza, Prof. J. Coronas, Prof. C. Téllez
Instituto de Nanociencia y Materiales de Aragón (INMA)
CSIC-Universidad de Zaragoza
Zaragoza, Zaragoza 50009 (Spain)
E-mail: bzornoza@unizar.es
ctellez@unizar.es

[b] Í. Martínez-Visus, M. Ulcuango, Dr. B. Zornoza, Prof. J. Coronas, Prof. C. Téllez
Chemical and Environmental Engineering Department
Universidad de Zaragoza
Zaragoza, Zaragoza 50018 (Spain)

Supporting information for this article is available on the WWW under https://doi.org/10.1002/chem.202203907

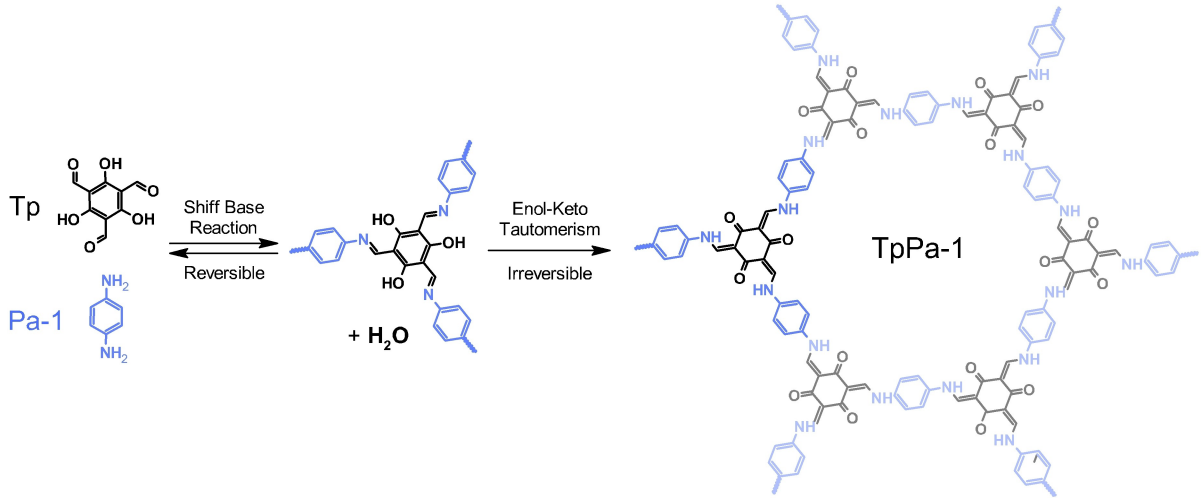

Figure 1. Schiff base reversible condensation reaction and irreversible enol-keto tautomerism forming an hexagonal framework of TpPa-1 obtained from monomers 1,3,5-triformylphloroglucinol (Tp) and *p*-phenylenediamine (Pa-1) in a stoichiometric ratio of 2:3.

microwave radiation in an organic solvent media gave rise to excellent properties at the same time that with the conventional solvothermal route.[25] Other Tp-based COFs with longer amines have been synthesized under microwave radiation in organic solvents.[26] The use of water as the solvent in microwave synthesis is rarer,[27,28] and there has not been any report of it in COF TpPa-1.

Herein, we report for the first time a fast and organic solvent-free microwave hydrothermal synthesis of TpPa-1, deemed a powerful tool for COF synthesis. In addition, three procedures for synthesizing TpPa-1 COF were compared: conventional hydrothermal synthesis (HT), microwave-assisted synthesis (MW) and mechanochemical synthesis (MC) which directly avoids the use of solvents. The methods were analyzed in terms of: i) their reaction times and temperatures used (allowing more energy-efficient processes), ii) the nature of the solvents employed (e.g., water, or non-solvent), iii) the use of a catalyst, iv) the textural properties, v) the crystallinity, and vii) the synthesis yields.

Results and Discussion

Three methods were used to carry out the study: hydrothermal synthesis, microwave-assisted hydrothermal synthesis and mechanochemical synthesis, denoted as TpPa-HT, TpPa-MW and TpPa-MC, respectively. Different synthesis conditions are tested, which are shown in Table 1 (see also Table S1 in the Supporting Information).

In the samples using optimized conditions for the three procedures, the crystalline framework of TpPa-1 features characteristic diffraction peaks at $2\theta = 4.7°$ (100), 8.1° (200), 12.7° (210) and 27.1° (001) (Figure 2), agreeing with previous reports for an eclipsed (AA) stacked structure.[29] As will be mentioned below, extensive research has been conducted proving that a parallel displaced AA stacking is the most stable configuration for the majority of 2D COFs, as opposed to a fully eclipsed one.[30]

Table 1. Range of synthesis conditions and yields with respect to reagent Pa-1 used in this study. Specific conditions and yields of each experiment can be found in Table S1.

Code	Method	*T* [°C]	Reaction time	Catalyst	Yield [%]
MC	mechano-chemical	120–190	1–60 min	PTSA	63–98
HT	hydrothermal	120–170	1–5 d	Acetic Ac.	82–90
MW	microwave-assisted	80–180	10–60 min	None, Acetic Ac.	70–99

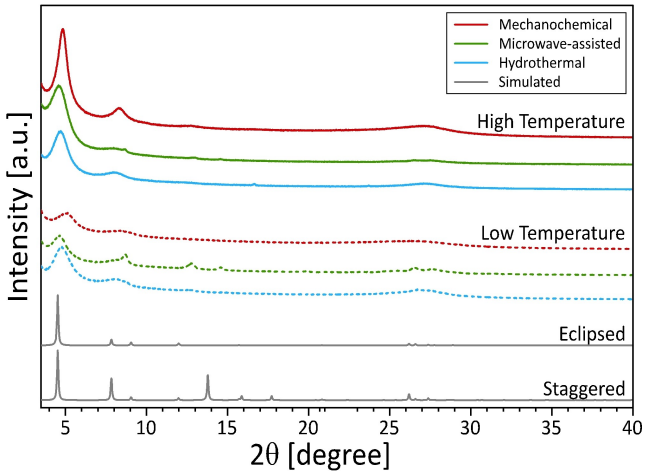

Figure 2. PXRD patterns of TpPa-1 formed by mechanochemical synthesis for 10 min, conventional hydrothermal synthesis for 3 days and microwave-assisted hydrothermal synthesis for 30 min at high and low temperatures. From top to bottom: MC/170 °C, MW/160 °C, HT/170 °C, MC/120 °C, MW/120 °C and HT/120 °C. At the bottom, simulated patterns of two different stacking modes of TpPa-1; the eclipsed stacked pattern was taken from ref. [31] by using Mercury 4.0.[32]

The water-assisted mechanochemically produced TpPa-1 was synthesized following a literature-reported method.[24] In the mechanochemical synthesis, the COF linking reagents are mixed in a mortar with p-toluene sulfonic acid (PTSA), which acts as a catalyst, and a small amount of water. After this mixing process, which lasts about 25 min, the solid mixture is introduced into an oven at different times and temperatures. The obtained solids were centrifuged and washed with a protocol that includes water, ethanol and acetone (details of the process can be seen in the experimental section). This cleaning process, used in all the synthesis procedures presented here, replaced the conventional DMAc washing with this more environmentally friendly alternative, showing a slight improvement in crystallinity (Figure S1). The optimal synthesis temperature for TpPa-MC was confirmed at 170 °C (Figure S2). No appreciable difference in PXRD patterns are detected between the 5 and 60 min synthesis time at 170 °C (Figure S3) and, in order to give the reaction enough time to finish, heating in the oven was set as optimum at 10 min. With the aim of increasing crystallinity and converting all reactants (Figure S4), a modified mechanochemical process was developed adding a second heating stage (see details in the Experimental Section), denoted TpPa-MC2.

The hydrothermal synthesis with conventional heating is carried out in an autoclave mixing the reagents in the aqueous phase with acetic acid, which acts as a catalyst in the formation of COF (see details in the Experimental Section). The optimal reaction time for hydrothermal synthesis was determined by analyzing the PXRD patterns for TpPa-HT at 120 °C (Figure S5), while the effect of synthesis temperature was studied under a reaction time duration of 3 days (Figure S6). The stoichiometric ratio of the reactants (Figure 1) was only maintained in optimal reaction time determination studies where the presence of unreacted Tp was observed by PXRD (Figure S5). In the subsequent hydrothermal syntheses, a stoichiometric excess of 50 % of Pa-1 was used instead, to make the most of the Tp (more expensive reactant).

Figure S5 shows that longer reaction times increased the peak intensities and yields of products. It is concluded that a minimum reaction time of 3 days was required to obtain the greatest XRD intensity for the 4.7° peak, indicating that the material crystallized better due to a more tightly packed 2D layer assembling. However, a longer reaction time than 5 days showed a drop of intensity in the PXRD peaks which could indicate a slight hydrothermal deterioration of the material. On the other hand, higher reaction temperatures achieved greater intensities for the 4.7° peak reaching the highest crystallinity for hydrothermally prepared COFs at 150 °C (Figure S6, inlaid graph) although very similar to that of 170 °C. It is precisely in the latter that the highest yield (of the limiting reagent up to 90 %, Tables 1 and S1) was reached. A broad peak at a high 2θ value of 27° is associated with the (001) diffraction plane, which directly relates the plane *d*-spacing to the π-π stacking distance between COF layers. By using Bragg's law, it is possible to determine the separation value between COF layers. An average value of 3.3 Å was calculated (Table S2) which was in accordance with other TpPa-1 *d*-spacing PXRD measurements in the literature.[33]

Microwave-assisted synthesis was developed under hydrothermal conditions analogously to conventional oven heating. It should be noted that with this type of heating, which is more efficient than conventional heating, the use of water as a solvent is unusual in the literature for COF synthesis.[27,34] MW synthesis was carried out at 80–180 °C reducing reaction times down to 30 min compared to HT synthesis, maintaining high yield and improving crystallinity by increasing synthesis temperature to 140–180 °C (Table S1 and Figure S7). By extending the reaction time up to an hour, the Tp reagent peak disappears from the diffractogram (Figure S8) and a 12 % yield gain (from 70 to 82 %) was accomplished for low temperature synthesis at 80 °C, while crystallinity was still subpar compared to that of the TpPa-MW produced at a higher temperature. Also, as seen in Figure S8, a minimum reaction time of 30 min was needed to ensure high crystallinity in microwave-assisted synthesis. Additionally, the measurement of the full-width at half-maximum (FWHM) revealed slightly wider peaks for the high temperature microwave-assisted synthesized COF compared to the conventionally heated TpPa-HT (Figure 2 and Table S2). This broadening may be attributed to smaller crystalline domain sizes caused by the enhancing effect of the microwave radiation used on the nucleation rate. Narrower particle distribution and accelerated synthesis of microporous materials through microwave synthesis have been proved. In opposition to conventional heating, it has been reported that microwave radiation speeds up particle nucleation and crystal growth in the synthesis of molecular sieves like zeolite silicalite-1 and nickel phosphate VSB-5.[35] Nevertheless, the microwave enhancement of the synthesis for nanoporous materials is not well understood, existing multiple hypotheses involving the higher heating rate, a more uniform heating, or a mixture of superheating and hotspot creation, among others.[36] In fact, different causes may take place simultaneously to provide a powerfully improved synthesis. In any case, compared to conventional HT synthesis, there has been a noticeable reduction time from days to hours or minutes, which is in agreement with what was found in other studies for different types of COF containing boronate ester; imine or triazine groups.[27]

As mentioned before, the PXRD patterns of the TpPa-1 obtained matched with layered stacking ordered in an eclipsed pattern instead of a staggered manner (Figure 2). As a result, hexagonal channels are created in the direction perpendicular to the basal plane. Also, stacked layers order themselves to minimize repulsion forces leading to alternating or staggered configurations.[37] Layers stacking in an offset-eclipsed manner can shift the hexagonal channel slope reducing the effective micropore radius.[38] However, no confirmation of this exact stack ordering can be inferred from the PXRD patterns of the synthesized solids.

The Fourier transform infrared spectroscopy of synthesized TpPa-1 in Figure 3A is in good agreement with published literature.[39] The absence of the distinctive carbonyl (C=O) stretching band (1635 cm^{-1}) of Tp and the characteristic free diamine N–H stretching (3371–3305 cm^{-1}) of Pa-1 in the

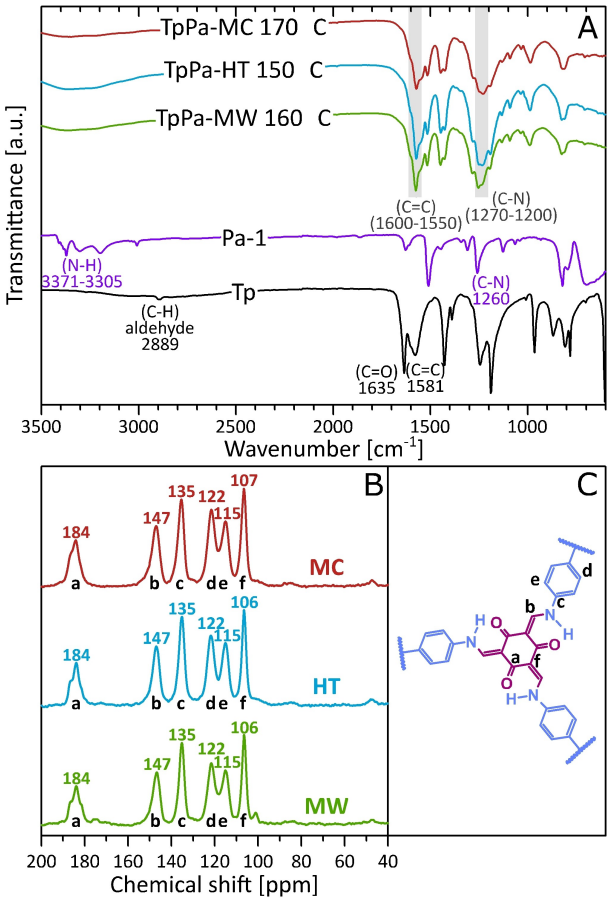

Figure 3. A) FTIR spectra of starting monomers (Tp and Pa-1) and COF TpPa-1 synthesized by different methods: mechanochemical synthesis (MC) at 170 °C for 10 min, hydrothermal synthesis (HT) at 150 °C and 3 d and microwave-assisted hydrothermal synthesis (MW) at 160 °C for 30 min. B) Comparison of the ^{13}C CP-MAS solid-state NMR spectra of TpPa-MC 170 °C (red), TpPa-HT 150 °C (blue) and TpPa-MW 160 °C (green). C) Assignment of ^{13}C NMR data (letters a-f).

produced solids supports the successful formation of the COF structure. The sharp peak at 1600–1550 cm^{-1}, which corresponds to the C=C stretching band, and the wider peak at 1270–1200 cm^{-1}, from the C–N enamine bond, confirm the keto-tautomeric form of the TpPa-1 produced within the three separate types of syntheses conducted. This finding is further supported by the fact that the enol form of the C=N imine bond cannot be detected by its expected stretching band at ~1690–1640 cm^{-1}. A small broad band at 3400–3100 cm^{-1} in the samples may be ascribed to the O–H bond from water adsorption. No discernible differences can be seen in the various spectra of TpPa-1 synthesized through different methods, as shown in Figure 3A and in more detail in Figure S9.

The correct formation of TpPa-1 structure was further confirmed by ^{13}C cross-polarization magic-angle spinning (CP-MAS) solid-state NMR spectroscopy (Figure 3B, C). Peaks in the range between 180 and 186 ppm are attributed to the carbonyl carbon (C=O, a), while the 147 ppm peak is assigned to the amine bond carbon (C–N, b). As neither characteristic enol aldehyde carbon (C–OH) nor imine carbon (C=N) peaks at 190 and 165 ppm were detected, the keto tautomeric form of TpPa-1 was confirmed.[30] Likewise, the ^{13}C NMR spectra of the three studied synthetic methods (Figure 3B) show virtually identical peak patterns, indicating that they all share the same chemical structure and are in good accordance with the literature.[40]

Thermogravimetric profile analysis (Figure 4) revealed high thermal stability for prepared TpPa-1 up to a temperature of 400 °C under a nitrogen atmosphere, maintaining more than 95 % weight of the sample. Higher temperatures than this value showed a 55 % total weight loss, which peaked at around 500 °C and is attributed to COF decomposition, in accordance with the literature.[31,41] Also, exposure to air atmosphere did not start degrading the material until 300 °C, reaching complete combustion of the COF at 650 °C as expected for organic materials. In any event, with the same atmosphere, the weight loss curves are, within the experimental error, quite similar even if the COFs were obtained by a different procedure (i.e., ST, MW or MC).

BET specific surface area (SSA) and porosity were determined from nitrogen sorption measurements (Figure 5). TpPa-1 synthesized by the two hydrothermal methods was identified as a combination of type I and IV adsorption isotherms following IUPAC classification,[42] presenting a minor hysteresis loop. Low relative pressure behavior points to micropore volume filling (< 2 nm), while the slower slope of the plateau is caused by multilayer adsorption on the smaller external surface of the material. Moreover, the hysteresis loop is commonly attributed to the existence of a mesoporous structure where capillary condensation takes place.[43] Also, this type of flat hysteresis loop within type I–IV isotherms is often associated with micro-mesoporous materials with narrow slit-like pores.[44] For the commonly used reaction temperature for TpPa-1 synthesis of 120 °C, BET SSA stayed low for TpPa-HT and TpPa-MW (440 and 266 m^2·g^{-1}). At higher temperatures greater BET SSA values were obtained, up to 1007 (HT) and 928 m^2·g^{-1}

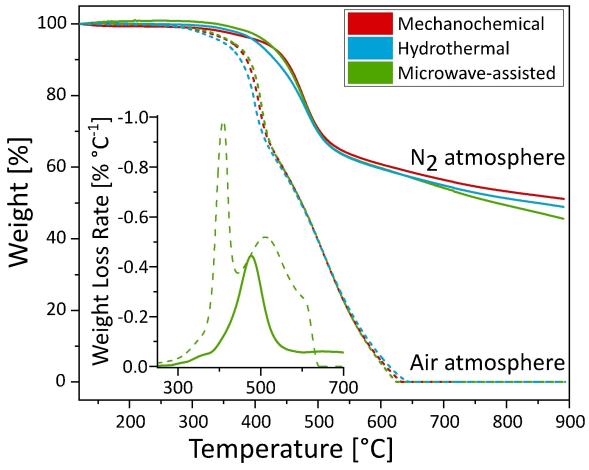

Figure 4. Thermogravimetric curves of TpPa-1 under N_2 and air atmospheres for the synthetic methods hydrothermal synthesis at 170 °C for 3 days, microwave-assisted synthesis at 160 °C for 30 min, and mechanochemical synthesis at 170 °C for 10 min. The weight loss rate for TpPa-1 microwave-assisted synthesis is shown in the inset graph.

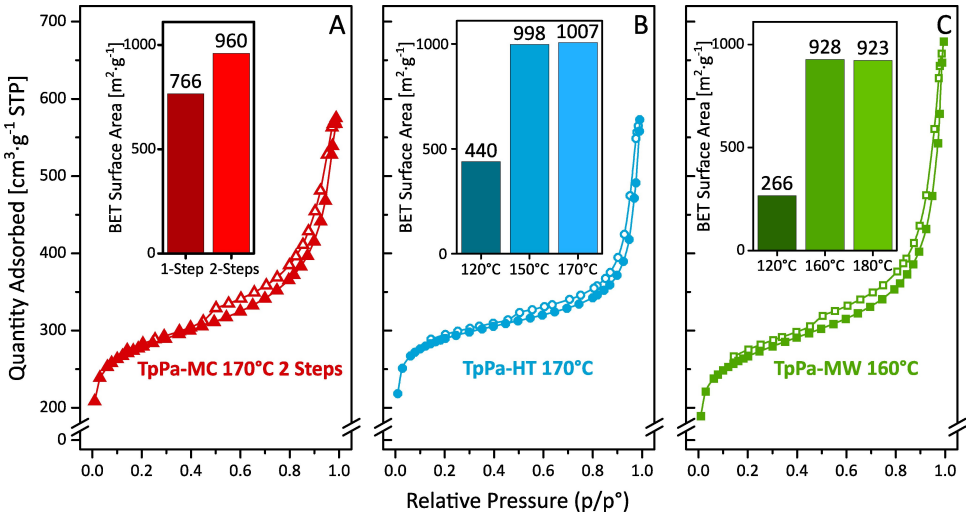

Figure 5. TpPa-1 nitrogen adsorption isotherms of COFs obtained by A) mechanochemical synthesis (TpPa-MC) at 170 °C for 2×10 min, B) hydrothermal synthesis (TpPa-HT) at 170 °C for 3 d, and C) microwave-assisted hydrothermal synthesis (TpPa-MW) at 160 °C for 30 min. BET specific surface areas for 1-step (10 min) and 2-step (2×10 min) TpPa-MC at 170 °C are shown in the first inset bar chart. For TpPa-HT (3 d) and TpPa-MW (30 min) synthesized at other temperatures BET SSA are shown in the inset bar charts.

(MW). Compared with the literature, these are the highest values reported for hydrothermally synthesized TpPa-1, as well as showing an improvement in BET SSA as compared to other conventional organic solvent-based solvothermal methods (Table 2).

Additionally, mechanochemically synthesized TpPa-MC at 170 °C achieved a BET SSA of 766 $m^2 \cdot g^{-1}$. Although it was lower than the reported value of the reference method (Table 2), the modified synthesis by incorporating two heating steps improved the value to 960 $m^2 \cdot g^{-1}$ (TpPa-MC2). Therefore, this improved method achieved a more consistent BET SSA comparable to those corresponding to both hydrothermal and microwave-assisted synthesis methods. Micropore surface area values determined by t-plot analysis (Harkins and Jura) were 747, 565, 508 and 638 $m^2 \cdot g^{-1}$ for TpPa-HT-170 °C, MW-180 °C, MC-170 °C and MC2-170 °C, respectively (Table S3), confirming the coexistence of both micro and mesoporosity in line with the shape of the isotherms. In general, hydrothermal synthesis of TpPa-1 at high temperatures (150 and 170 °C) had the highest BET SSA values and micropore surface areas (at 170 °C).

In the conventional procedure, the usage of organic solvents promotes a monomer condensation in the equilibrium reaction, inhibiting the reversibility of covalent bonds and decreasing the overall quality of the material. Smith et al.[47] did a mechanistic study of an imine-linked COF showing that a minimum amount of water and acetic acid was required to avoid the formation of low crystallinity powders. To confirm this requirement, MW syntheses without the presence of acetic acid were carried out at high and low temperatures. TpPa-MW prepared in absence of catalyst at 180 °C produced a poor BET SSA (258 $m^2 \cdot g^{-1}$), as well as lower intensities in its PXRD pattern compared with its catalyzed counterpart (Figure S10). Therefore, it has been established that a catalyst like acetic acid is required

Table 2. Comparison of operating conditions and BET SSA values corresponding to the synthesis of COF TpPa-1.

Method	Solvents	Operating conditions		S_{BET} [$m^2 \cdot g^{-1}$]	Ref.
		T [°C]	t		
solvothermal	1:1 mesitylene/dioxane	120	3 d	535	[31]
solvothermal	1:1 mesitylene/dioxane	120	3 d	421	[45]
solvothermal	1:1 mesitylene/dioxane	120	3 d	600	[29]
solvothermal	1:1 mesitylene/dioxane	100	1 h	153	[25]
microwave-assisted	1:1 mesitylene/dioxane	100	1 h	725	[25]
hydrothermal	water	120	3 d	633	[23]
hydrothermal	water	170	3 d	1007	this work
microwave-assisted	water	160	30 min	928	this work
mechanochemical	water	170	10 min	766	this work
mechanochemical[a]	water	170	20 min	960	this work
mechanochemical	water	170	1 min	1432	[24]
solution-suspension	dioxane	RT[b]	3 d	834	[46]
solution-suspension	deep eutectic solvent	RT[b]	2 h	977	[41]

[a] Modified synthetic procedure with two heating phases of 10 min each with grinding in between. [b] Room temperature.

to produce an ordered structure, accessible pores and high crystallinity.[48]

Among the used tactics for achieving high-quality COFs[12] (such as modulation, improved catalysts or exchange reactions) monomer availability and solubility effects may be the cause of the major enhancement in textural properties of TpPa-1 obtained at higher reaction temperatures. Usually, a good solubility control of the monomers is achieved thanks to the wide selection of solvents and their possible ratios (although through a trial-and-error process). However, there is less room for maneuver in a water-based synthesis as the aldehyde linker is poorly soluble at ambient temperature, whereas organic solvents are more suitable. Even though a lower availability of monomer promotes the formation of an ordered structure with fewer defects, an aldehyde saturated solution might inhibit the reverse Schiff reaction leading to a more amorphous solid. Therefore, synthesis under high temperatures could be beneficial in two ways: i) thermodynamically, by increasing the maximum capacity of soluble Tp monomer improving reversibility, and ii) kinetically, by speeding up both forward and backward reactions allowing a faster reassembly correction into an ordered structure.[49] On the other hand, the irreversible enol-keto tautomerism is slightly favored at higher temperatures, leading to an unwanted crystallization before a sorted structure is achieved. For instance, pentane-1,3,5-triones are significantly favored to keto tautomerization in polar solvents at high temperatures (140 °C). While 2-phenacylquinolines are in a chloroform solution, its enol tautomeric form is promoted by the presence of deprotonators and low temperatures. However, once temperatures rise beyond 300 K, the effect of deprotonator concentration on the enol-keto ratio is significantly reduced.[50]

An important aspect that was observed during the synthesis process is related to the contact time spent by the reactants before heating up to the desired reaction temperature. After adding the reactants to the solution, stirring is needed and a certain time passes while transferring it into the autoclave (TpPa-HT) or the microwave vessel (TpPa-MW). During this step, a change in the color of the solution can be seen with the naked eye, indicating that a quick reaction is taking place at room temperature. A rapid formation of stable oligomers within the first seconds of the mixture between Pa-1 and Tp has been detected in the literature, promoting the formation of a more densely packed and crystalline material.[51] Furthermore, under room temperature conditions, π-π stacking interactions between monomers and oligomers seem to be a key driving force in achieving high crystalline COFs.[46] Similarly, in the case of TpPa-MC synthesis, the 10-minute grinding step that ensures an intimate mixture of monomers and catalyst was confirmed as an essential step of COF molecular self-organization before the heating process, giving rise to high crystallinity and SSA.[24]

SEM and TEM imaging showed fibrous thread-like particles with an average width of 50 nm (Figure 6c–f) which also were observed across hydrothermal samples obtained from low to high temperatures. This is consistent with the literature, as the presence of higher water content in the solvothermal preparation of TpPa-1 produced filaments and plate-like morphologies instead of spherical flower-like particles.[29] The hydrothermal method at 120 °C gave rise to a predominant morphology of big-sized ball aggregates with a wide range of diameters from 500 nm up to 2 μm (Figure 6a, b). Mechanochemical synthesis was confirmed to preferably yield more 2D stacked morphologies than hydrothermal methods as well as larger sized aggregates,[17,31] although stacked flat plate particles were also

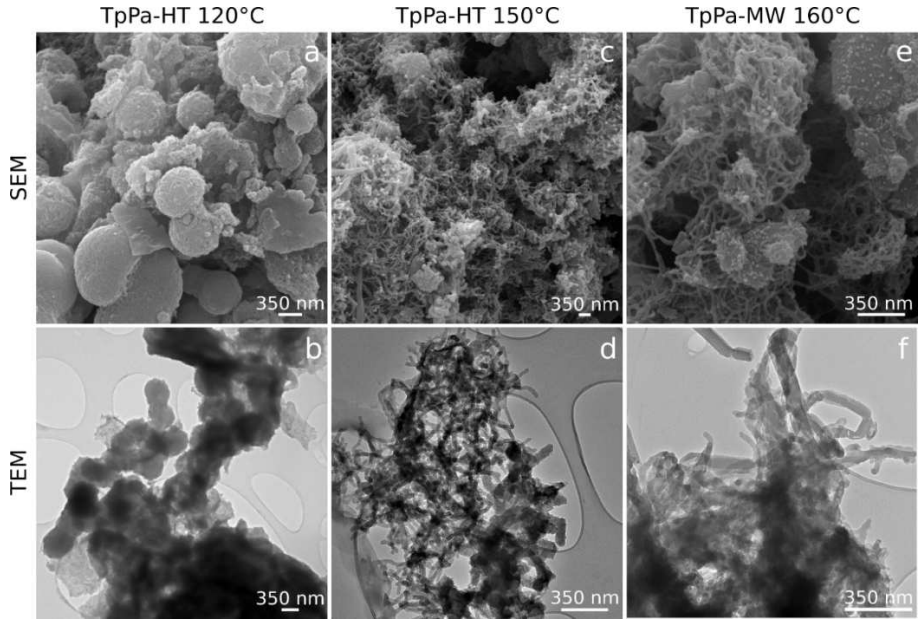

Figure 6. Different morphologies of TpPa-1 obtained by hydrothermal and microwave-assisted syntheses: fibrous threads (c–f), sphere shaped (a, b) and plate-like (a, e), observed by SEM (top row) and TEM (bottom row) imaging. Samples of TpPa-HT prepared at 120 °C for 3 d (first column), TpPa-HT at 150 °C for 3 d (second column) and TpPa-MW at 160 °C for 30 min (third column).

present in TpPa-ST and TpPa-MW but to a lesser extent as seen in Figure 6e. Not enough reaction time resulted in big bulky agglomerates and half-formed thread particles as observed by SEM analysis (Figure S13). Also, worse crystallinity and lower BET SSA values were obtained compared to the longer reaction time counterpart.

The filamentous particles produced by conventional heating were substantially shorter and thinner than those created by microwave synthesis, as can be seen in Figure S11 and TEM images of Figure 6d, f. It is possible that the faster aggregation and crystal growth of the material is what causes the shift in morphology from sphere-like particles to smaller nanothreads by increasing reaction temperature. Interestingly, another β-ketoenamine COF in the literature also exhibited a similar thread-like shape at high temperatures.[52] Also, SEM-TEM imaging indicates the existence of an intriguing microwave effect at high temperatures for the TpPa-1 synthesis. Microwave radiation aids a rapid nucleation and then growth in the axial direction of the particles, forming long tangled threads that allow the shaping of the observed fibrous network with rich surface texture and mesoporosity. Also, by TEM imaging, these long threads were seen ordering themselves into larger flat-like structures (Figure S12). Similar to the behavior observed at different stages of the reported "organic terracotta process" where a fibrous network forms first and develops into bigger sheets.[24]

As previously stated, higher temperatures and water as solvent provide benefits for better crystallinity and high BET SSAs. In addition, MW synthesis at 180 °C did not impede the nanosheet formation, as observed by electron microscopy analysis finding 2D sheets as well as micrometer-sized stacked plates. Furthermore, recent evidence has been found by Feriante et al.[53] about the formation mechanism of 2D imine-linked COFs. Longer reaction times, used for enabling the COF amorphous-to-crystalline transition, mask the formation and detection of highly crystalline sheets in the first minutes of solvothermal synthesis. This fast polymerization is compatible with short reaction times, which could be achieved by microwave-assisted synthesis.

Conclusion

In this work, it has been shown that TpPa-1 can be synthesized by microwave hydrothermal synthesis with morphology, crystallinity and textural properties similar to those obtained with both conventional-heating hydrothermal and mechano-chemical syntheses. Furthermore, synthesis by microwave radiation has the advantages of a shorter reaction time and lower energy cost with higher yields.

By increasing the usual synthesis temperature of 120 °C to 170 °C, the hydrothermal synthesis improved TpPa-1's crystallinity and BET specific surface areas, imitating the effects of other procedures such as mechanochemical methods. Additionally, synthesis yields were increased by using microwave heating, which also preserved the crystallinity and specific surface areas and cut reaction times from 3 days down to only 30 min. For both synthetic processes, TpPa-1 grew as fibrous threads rather than larger ball-like particles when exposed to high temperatures during synthesis. For high-temperature conventionally heated hydrothermal synthesis, these threads grew considerably less than their microwave-assisted counterpart. Alternatively, modification of the mechanochemical procedure by a two-step heating process clearly improved textural properties. In general, the use of a proton donator as a catalyst was confirmed as essential for achieving a highly ordered framework by enabling the reorganization of the structure. With the optimal reaction conditions, synthetic procedures were able to yield crystalline materials with similar high BET specific surface areas.

In summary, this work opens the door to the synthesis of COFs under more environmentally friendly conditions by using water as reaction medium and nontoxic solvents for washing. Microwave radiation has been shown to be a more energy-efficient heating alternative capable of lowering reaction times while maintaining the textural, crystalline and morphology properties of the materials.

Experimental Section

Materials: Monomer 2,4,6-triformylphloroglucinol (Tp, 97%) was purchased from ET Co. Ltd. and 1,4-phenylelendiamine (Pa-1, >98%) was provided by Tokyo Chemical Industry. Glacial acetic acid (≥99.8%) and *p*-toluenesulfonic acid monohydrate (PTSA, ≥98%) were purchased from Fisher Scientific and Sigma Aldrich, respectively. As solvents, dimethylacetamide (DMAc, 99%) was supplied by Alfa Aesar, while deionized water, ethanol and acetone were provided by Productos Gilca SC.

Mechanochemical synthesis of TpPa-1: Following a literature-reported method,[24] PTSA (951 mg) was taken in a mortar and broken down with the pestle into smaller chunks. Pa-1 (97.2 mg) was added and mixed thoroughly in the mortar for 5 min with the catalyst. Then Tp (126 mg) was added, and the compounds were mixed for 10 min until they turned a lighter pink. Afterwards, 200 μL of distilled water was added dropwise and continuously mixed for at least 10 min more; a pale-yellow mud was obtained. The mixture was spread onto a flat ceramic crucible and was put into a preheated oven at the desired temperature (120–190 °C) and time (1 to 60 min). The solidified mud was collected and grounded in the mortar before the optimal washing-centrifugation cycles were carried out. Optimal washing cycles used 3 washes in water, 1 in ethanol and 1 last wash in acetone. For the washes with water, the solids were added in a recipient with 50 mL of water and were kept at 80 °C for 10 min under agitation. As for ethanol, a round bottom flask and 80 mL of ethanol was used with reflux for 12 h at 80 °C. A final wash at room temperature in acetone was applied for 10 min, after which the centrifuged solids were dried overnight at 120 °C for complete elimination of solvents. The red solids obtained were denoted TpPa-MC.

With the aim of increasing crystallinity and converting all reactants, a modified mechanochemical process was developed adding a second heating stage. First, following the initial 10 min of heating in the oven, the solidified cmud was grounded in a mortar and then rehydrated with another 200 μL of distilled water. Subsequently, the powder was thoroughly mixed for 2 min, transferred again into a ceramic crucible and heated for another 10 min. Finally, the aforementioned washing-centrifugation cycles and drying were carried out, obtaining a red solid denoted as TpPa-MC2.

Hydrothermal synthesis: For the synthesis of TpPa-HT, a glass beaker was filled with 18 mL of distilled water and Pa-1 (93.8 mg), and the mixture was left stirring for 5 min until complete dissolution. Afterwards, Tp (81.0 mg) and 9 mL of glacial acetic acid (≥99.8%) were stirred for a further 5 min. Then, the suspension was transferred to two 15 mL PTFE lined autoclaves and left in a oven at the desired temperature (100–170 °C) and time (1 to 5 days) with a heating rate of 5 °C·min^{-1}. After synthesis, the autoclaves were cooled down to room temperature before the red powder was retrieved. The obtained solids were centrifuged at 9000 rpm for 10 min, following multiple washing cycles as aforementioned. The bright red powders were then collected in a vial and denoted TpPa-HT with a yield of 76–90%.

Microwave-assisted hydrothermal synthesis: TpPa-MW was carried out similarly to the aforementioned hydrothermal synthesis. Pa-1 (93.8 mg) was dissolved in distilled water (18 mL) in a glass beaker under magnetic stirring for 5 min. After complete dissolution of the amine, Tp (81.0 mg) and glacial acetic acid (≥99.8%, 9 mL) were added and mixed for 5 min more. Then, the suspension was transferred to a sealed 100 mL PTFE tube with a magnetic stir bar into an Anton Paar Multiwave 3000 microwave apparatus. The desired temperature (80–180 °C) was maintained for 30 min using a thermocouple inside the solution with a heating rate of 1 °C·s^{-1}. Subsequently, the same washing protocol described above was followed for the centrifugation-washing cycles with water, ethanol and acetone. The solid collected with 70–99% yield was dried overnight at 120 °C and denoted as TpPa-MW.

Characterization of materials: Powder X-ray diffraction (PXRD) measurements of the synthesized powders were performed using a reflection-transmission spinner stage with a zero-background sample holder on PANalytical Emphyrean-Multipurpose ($Cu_{K\alpha}$). Nitrogen adsorption-desorption isotherms at −195.8 °C were acquired with a Micromeritics TriStar 3000 apparatus. The samples were previously degassed at 200 °C for 12 h in a Micromeritics VacPrep™ 061. Field-emission scanning electron microscopy (SEM) and transmission electron microscopy (TEM) images were obtained using an Inspect F50 model scanning electron microscope (FEI, operated at 10 kV) and a Tecnai G2 T20 (FEI, 200 kV), respectively. Samples were firstly dispersed in water by sonication in an ultrasound bath. The obtained suspension was left to settle for 5 min, and the supernatant was used for drop-casting onto the sample holders. Thermogravimetric analysis (TGA) for thermal stability determination was performed with a Mettler Toledo GA/STDA 851e. A small amount of COF powder (~4 mg) placed in a 70 μL alumina crucible was heated from 35 to 900 °C at a heating rate of 10 °C·min^{-1}. The analyses were performed under N_2 as well as under synthetic air (30 cm^3(STP)·min^{-1}). FTIR was conducted with a Bruker Vertex 70 FTIR provisioned with a DTGS detector and a Golden Gate diamond attenuated total reflectance (ATR) accessory. The spectra were recorded by averaging 40 scans in the 4000–600 cm^{-1} wavenumber range at a resolution of 4 cm^{-1}. Solid-state cross-polarization magic angle spinning (CP MAS) ^{13}C NMR spectra were acquired with a Bruker Avance III 400 MHz Wide Bore spectrometer equipped with a 4 mm CP MAS 1H-BB probe. Approximately 100 mg of the material was packed in a 4 mm zirconium rotor and sealed with a Kel-F cap. Spectra were acquired with a MAS rate of 10 kHz, a ramp-CP contact time of 3 ms and a 7 s recycle delay.

Acknowledgements

This research gratefully acknowledges grant PID2019-104009RB–I00 funded by MCIN/AEI/10.13039/501100011033 (Agencia Estatal de Investigación (AEI) and Ministerio de Ciencia e Innovación (MCIN), Spain). Grant PRE2020-092006 funded by MCIN/AEI/ 10.13039/501100011033 and by "ESF Investing in your future" is gratefully acknowledged by Í. Martínez-Visus. The authors would like to acknowledge the use of Servicio General de Apoyo a la Investigación-SAI, Universidad de Zaragoza, and the use of instrumentation as well as the technical advice provided by the National Facility ELECMI ICTS, node «Laboratorio de Microscopias Avanzadas (LMA)» at Universidad de Zaragoza.

Conflict of Interest

The authors declare no conflicts of interest.

Data Availability Statement

Most of the data that support the findings of this study are available in the Supporting Information for this article, other data from this study are available from the corresponding author upon reasonable request.

Keywords: covalent-organic frameworks · green chemistry · hydrothermal synthesis · microwave chemistry · TpPa-1

[1] A. P. Côté, A. I. Benin, N. W. Ockwig, M. O'Keeffe, A. J. Matzger, O. M. Yaghi, *Science* **2005**, *310*, 1166–1170.
[2] S. Y. Ding, W. Wang, *Chem. Soc. Rev.* **2013**, *42*, 548–568.
[3] J. L. Segura, S. Royuela, M. Mar Ramos, *Chem. Soc. Rev.* **2019**, *48*, 3903–3945.
[4] B. Sun, C.-H. Zhu, Y. Liu, C. Wang, L.-J. Wan, D. Wang, *Chem. Mater.* **2017**, *29*, 4367–4374.
[5] M. G. Rabbani, A. K. Sekizkardes, Z. Kahveci, T. E. Reich, R. Ding, H. M. El-Kaderi, *Chem. Eur. J.* **2013**, *19*, 3324–3328.
[6] S. Yuan, X. Li, J. Zhu, G. Zhang, P. V. Puyvelde, B. V. d. Bruggen, *Chem. Soc. Rev.* **2019**, *48*, 2665–2681.
[7] Y. Peng, Z. Hu, Y. Gao, D. Yuan, Z. Kang, Y. Qian, N. Yan, D. Zhao, *ChemSusChem* **2015**, *8*, 3208–3212.
[8] S. Liu, M. Tian, X. Bu, H. Tian, X. Yang, *Chem. Eur. J.* **2021**, *27*, 7738–7744.
[9] B. P. Biswal, H. D. Chaudhari, R. Banerjee, U. K. Kharul, *Chem. Eur. J.* **2016**, *22*, 4695–4699.
[10] Q. Fang, J. Wang, S. Gu, R. B. Kaspar, Z. Zhuang, J. Zheng, H. Guo, S. Qiu, Y. Yan, *J. Am. Chem. Soc.* **2015**, *137*, 8352–8355.
[11] F. J. Uribe-Romo, J. R. Hunt, H. Furukawa, C. Klöck, M. O'Keeffe, O. M. Yaghi, *J. Am. Chem. Soc.* **2009**, *131*, 4570–4571.
[12] L. Bourda, C. Krishnaraj, P. Van Der Voort, K. Van Hecke, *Mater Adv* **2021**, *2*, 2811–2845.
[13] S. Kandambeth, A. Mallick, B. Lukose, M. V. Mane, T. Heine, R. Banerjee, *J. Am. Chem. Soc.* **2012**, *134*.
[14] K. Geng, T. He, R. Liu, S. Dalapati, K. T. Tan, Z. Li, S. Tao, Y. Gong, Q. Jiang, D. Jiang, *Chem. Rev.* **2020**, *120*, 8814–8933.
[15] P. Kuhn, M. Antonietti, A. Thomas, *Angew. Chem. Int. Ed.* **2008**, *47*, 3450–3453; *Angew. Chem.* **2008**, *120*, 3499–3502.
[16] D. Hao, J. Zhang, H. Lu, W. Leng, R. Ge, X. Dai, Y. Gao, *Chem. Commun.* **2014**, *50*, 1462–1464.
[17] B. P. Biswal, S. Chandra, S. Kandambeth, B. Lukose, T. Heine, R. Banerjee, *J. Am. Chem. Soc.* **2013**, *135*, 5328–5331.
[18] L. Y. Chen, Y. N. Gai, X. T. Gai, J. Qin, Z. G. Wang, L. S. Cui, H. Guo, M. Y. Jiang, Q. Zou, T. Zhou, J. G. Gai, *Chem. Eng. J.* **2022**, *430*, 133024–133024; T. Wang, H. Wu, S. Zhao, W. Zhang, M. Tahir, Z. Wang, J. Wang, *Chem. Eng. J.* **2020**, *384*.
[19] J. L. Segura, M. J. Mancheño, F. Zamora, *Chem. Soc. Rev.* **2016**, *45*, 5635–5671.

[20] L. K. Ritchie, A. Trewin, A. Reguera-Galan, T. Hasell, A. I. Cooper, *Microporous Mesoporous Mater.* **2010**, *132*, 132–136; N. L. Campbell, R. Clowes, L. K. Ritchie, A. I. Cooper, *Chem. Mater.* **2009**, *21*, 204–206.
[21] W. Zhao, P. Yan, H. Yang, M. Bahri, A. M. James, H. Chen, L. Liu, B. Li, Z. Pang, R. Clowes, N. D. Browning, J. W. Ward, Y. Wu, A. I. Cooper, *Nat. Synth.* **2022**, *1*, 87–95.
[22] Z. Wang, Y. Yang, Z. Zhao, P. Zhang, Y. Zhang, J. Liu, S. Ma, P. Cheng, Y. Chen, Z. Zhang, *Nat. Commun.* **2021**, *12*, 1982.
[23] J. Thote, H. Barike Aiyappa, R. Rahul Kumar, S. Kandambeth, B. P. Biswal, D. Balaji Shinde, N. Chaki Roy, R. Banerjee, *IUCrJ* **2016**, *3*, 402–407.
[24] S. Karak, S. Kandambeth, B. P. Biswal, H. S. Sasmal, S. Kumar, P. Pachfule, R. Banerjee, *J. Am. Chem. Soc.* **2017**, *139*, 1856–1862.
[25] H. Wei, S. Chai, N. Hu, Z. Yang, L. Wei, L. Wang, *Chem. Commun.* **2015**, *51*, 12178–12181.
[26] T. F. Machado, F. A. Santos, R. F. P. Pereira, V. de Zea Bermudez, A. J. M. Valente, M. E. Serra, D. Murtinho, *Polymer* **2022**, *14*, 3096.
[27] B. Díaz de Greñu, J. Torres, J. García-González, S. Muñoz-Pina, R. de los Reyes, A. M. Costero, P. Amorós, J. V. Ros-Lis, *ChemSusChem* **2021**, *14*, 208–233.
[28] J. Á. Martín-Illán, D. Rodríguez-San-Miguel, C. Franco, I. Imaz, D. Maspoch, J. Puigmartí-Luis, F. Zamora, *Chem. Commun.* **2020**, *56*, 6704–6707.
[29] R. Chen, F. Wang, J. Zhang, Y. Shao, H. Jiang, Y. Liu, *Ind. Eng. Chem. Res.* **2020**, *59*, 18489–18499.
[30] S. Chandra, S. Kandambeth, B. P. Biswal, B. Lukose, S. M. Kunjir, M. Chaudhary, R. Babarao, T. Heine, R. Banerjee, *J. Am. Chem. Soc.* **2013**, *135*, 17853–17861.
[31] S. Kandambeth, A. Mallick, B. Lukose, M. V. Mane, T. Heine, R. Banerjee, *J. Am. Chem. Soc.* **2012**, *134*, 19524-19527.
[32] C. F. Macrae, I. Sovago, S. J. Cottrell, P. T. A. Galek, P. Mccabe, E. Pidcock, M. Platings, G. P. Shields, J. S. Stevens, M. Towler, P. A. Wood, *J. Appl. Crystallogr.* **2020**, *53*, 226–235.
[33] Y. Wang, P. Dong, K. Zhu, A. Zhang, J. Pan, Z. Chen, Z. Li, R. Guan, X. Xi, J. Zhang, *Chem. Eng. J.* **2022**, *446*, 136883.
[34] J. Xiao, J. Chen, J. Liu, H. Ihara, H. Qiu, *Green Energy & Environ.* **2022**.
[35] S. H. Jhung, T. Jin, Y. K. Hwang, J. S. Chang, *Chem. Eur. J.* **2007**, *13*, 4410–4417.
[36] G. A. Tompsett, W. C. Conner, K. S. Yngvesson, *ChemPhysChem* **2006**, *7*, 296–319.
[37] B. Lukose, A. Kuc, T. Heine, *Chem. Eur. J.* **2011**, *17*, 2388–2392.
[38] W. Zhou, M. Wei, X. Zhang, F. Xu, Y. Wang, *ACS Appl. Mater. Interfaces* **2019**, *11*, 16847–16854.
[39] P. Pachfule, M. K. Panda, S. Kandambeth, S. M. Shivaprasad, D. D. Díaz, R. Banerjee, *J. Mater. Chem. A* **2014**, *2*, 7944–7952.
[40] J. Ma, X.-B. Fu, Y. Li, T. Xia, L. Pan, Y.-F. Yao, *Microporous Mesoporous Mater.* **2020**, *305*, 110287; X. Zhong, W. Liang, Z. Lu, B. Hu, *Appl. Surf. Sci.* **2020**, *504*, 144403.
[41] J. Qiu, P. Guan, Y. Zhao, Z. Li, H. Wang, J. Wang, *Green Chem.* **2020**, *22*, 7537–7542.
[42] M. Thommes, K. Kaneko, A. V. Neimark, J. P. Olivier, F. Rodriguez-Reinoso, J. Rouquerol, K. S. W. Sing, *Pure Appl. Chem.* **2015**, *87*, 1051–1069.
[43] K. S. W. Sing, D. H. Everett, R. A. W. Haul, L. Moscou, R. A. Pierotti, J. Rouquerol, T. Siemieniewska, *Pure Appl. Chem.* **1985**, *57*, 603–619.
[44] R. Bardestani, G. S. Patience, S. Kaliaguine, *Can. J. Chem. Eng.* **2019**, *97*, 2781–2791.
[45] P. Wang, Y. Peng, C. Zhu, R. Yao, H. Song, L. Kun, W. Yang, *Angew. Chem.* **2021**, *133*, 19195–19200; *Angew. Chem. Int. Ed.* **2021**, *60*, 19047–19052.
[46] Y. Peng, W. K. Wong, Z. Hu, Y. Cheng, D. Yuan, S. A. Khan, D. Zhao, *Chem. Mater.* **2016**, *28*, 5095–5101.
[47] B. J. Smith, A. C. Overholts, N. Hwang, W. R. Dichtel, *Chem. Commun.* **2016**, *52*, 3690–3693.
[48] D. M. Fischbach, G. Rhoades, C. Espy, F. Goldberg, B. J. Smith, *Chem. Commun.* **2019**, *55*, 3594–3597.
[49] T. Sun, Y. Liang, Y. Xu, *Angew. Chem. Int. Ed.* **2022**, *61*, e202113926-e202113926.
[50] E. Kolehmainen, B. Ośmialowski, T. M. Krygowski, R. Kauppinen, M. Nissinen, R. Gawinecki, *J. Chem. Soc. Perkin Trans. 2* **2000**, *6*, 1259–1266.
[51] R. Lei, Z. Zha, Z. Hao, J. Wang, Z. Wang, S. Zhao, *J. Membr. Sci.* **2022**, *650*, 120431–120431.
[52] W. Zhao, J. Qiao, T.-L. Ning, X.-K. Liu, *Chin. J. Polym. Sci.* **2018**, *36*, 1–7.
[53] C. Feriante, A. M. Evans, S. Jhulki, I. Castano, M. J. Strauss, S. Barlow, W. R. Dichtel, S. R. Marder, *J. Am. Chem. Soc.* **2020**, *142*, 18637–18644.

Manuscript received: December 14, 2022
Accepted manuscript online: January 18, 2023
Version of record online: February 9, 2023